Microwave and Millimeter-wave Cavity R&D at SLAC

Emilio A. Nanni

August 27, 2015

U.S. DEPARTMENT OF ENERGY
Office of Science

SLAC NATIONAL ACCELERATOR LABORATORY

Acknowledgements

Majority of work shown from SLAC:

Sami Tantawi

Craig Burkhart

Paul Welander

Matt Franzi

Valery Dolgashev

Temkin Group:

Rick Temkin, Paul Woskov, Michael Shapiro, Roark Marsh, Brian Munroe, Sudheer Jawla and Samantha Lewis

Technologies of Interest to Axion Community

Coupled Cavity Structures

Mode Selective Cavities

Low Loss Waveguides and Cavities

Low Temperature Surface Resistivity Measurements

Technologies of Interest to Axion Community

SLAC

Coupled Cavity Structures

Mode Selective Cavities

Low Loss Waveguides and Cavities

Low Temperature Surface Resistivity Measurements

Accelerating Structures with Distributed Coupling

- Standing wave accelerating structures with distributed coupling could be adapted for Axion search
  - Use electron beam tunnel for perturbation to tune cavities actively
- Historically coupling was … interesting

Tantawi, Sami G., et al. "Research and development for ultra-high gradient accelerator structures." *AIP Conference Proceedings*. Vol. 1299. No. 1. 2010.

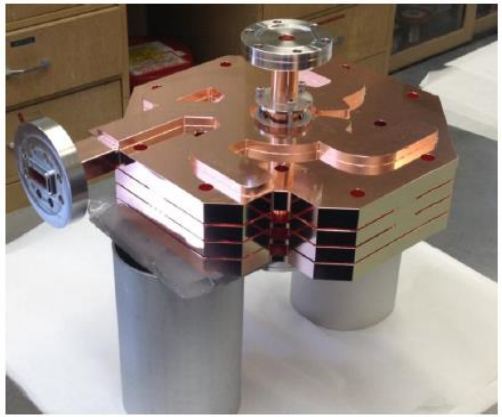

Standing Wave Coupled Cavity Structures

- New approach under test at SLAC much more compact

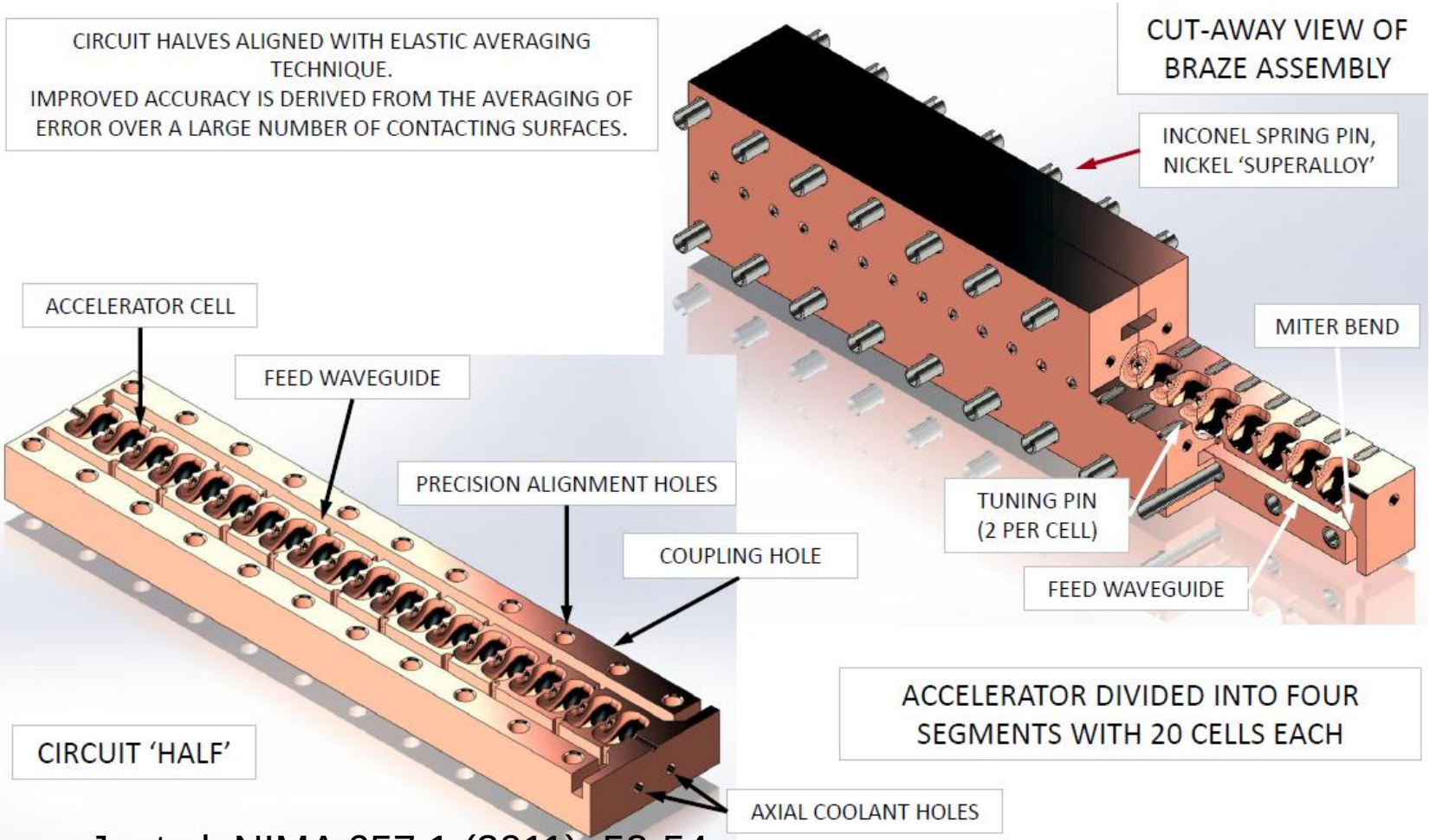

Neilson, J. et al. NIMA 657.1 (2011): 52-54.

S. Tantawi Qatar Foundation Workshop on Compact X-ray Light Sources 2014

Technologies of Interest to Axion Community

SLAC

Coupled Cavity Structures

Mode Selective Cavities

Low Loss Waveguides and Cavities

Low Temperature Surface Resistivity Measurements

Mode Suppression in Accelerating Structures

- Mode competition is a major concern in accelerators
- Major efforts to develop cavities that suppress undesired modes

- One approach is to add damping with cells or couplers to remove power from problematic modes

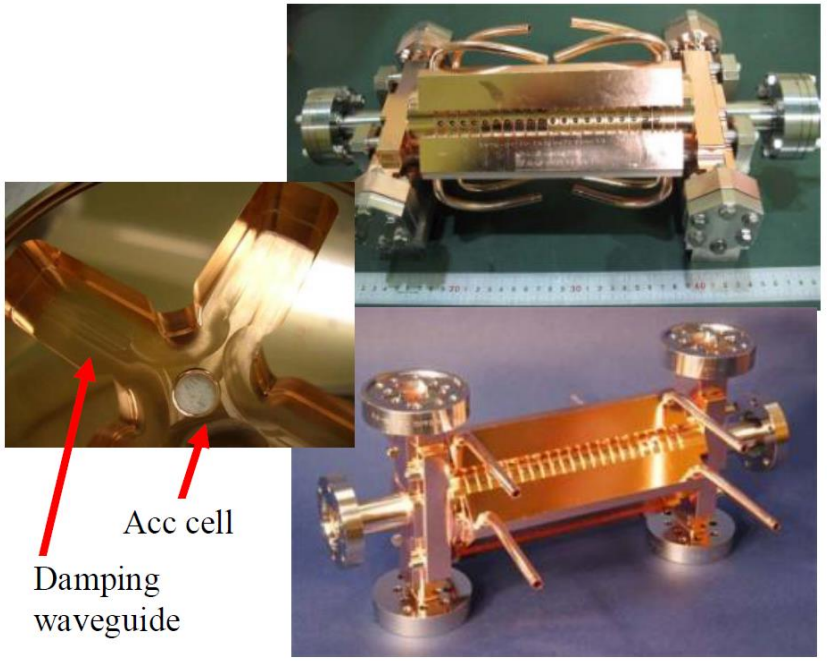

Higo, Toshiyasu, et al. "Advances in X-band TW Accelerator Structures Operating in the 100 MV/m Regime." *THPEA013, IPAC10, Kyoto* (2010).

PBG Cavities for Mode Selectivity

- PBG Cavities can be used to damp TE and TM modes that are not of interest
- Structures built from GHz to 100's of GHz

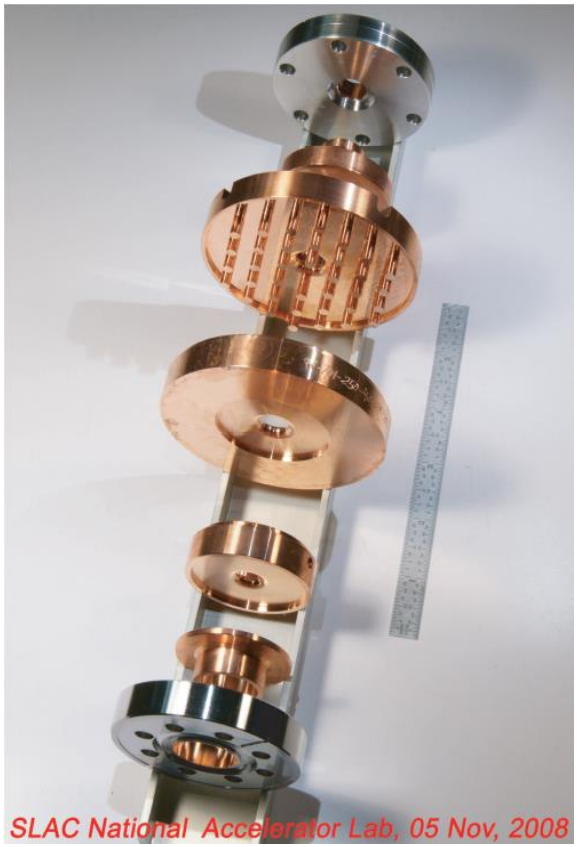

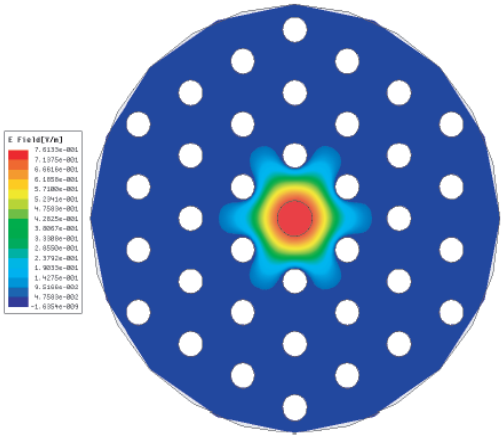

TM Modes

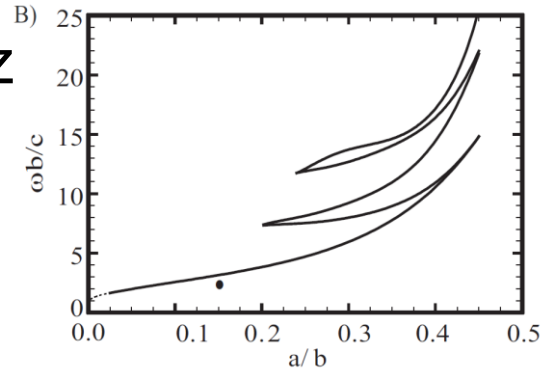

TE Modes

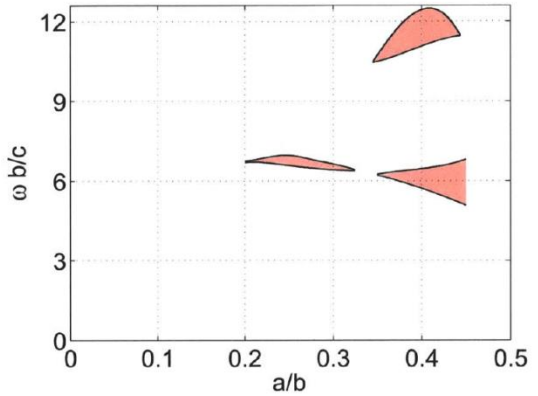

Marsh, Roark A. Diss. MIT, 2009.
Munroe, Brian J., et al. *PRST-AB* 16.1 (2013): 012005.
Nanni, E. A., et al. PRL 111.23 (2013): 235101.

Technologies of Interest to Axion Community

SLAC

Coupled Cavity Structures

Mode Selective Cavities

Low Loss Waveguides and Cavities

Low Temperature Surface Resistivity Measurements

Overmoded Corrugated Waveguide

- HE_{11} mode in metallic corrugated waveguide as very low loss and wide bandwidths
- Radius a >> λ, Groove depth d ≈ λ/4, Period p ≈ λ/3 and Groove Width w < p/2
- Use helical tapping to overcome fabrication challenges

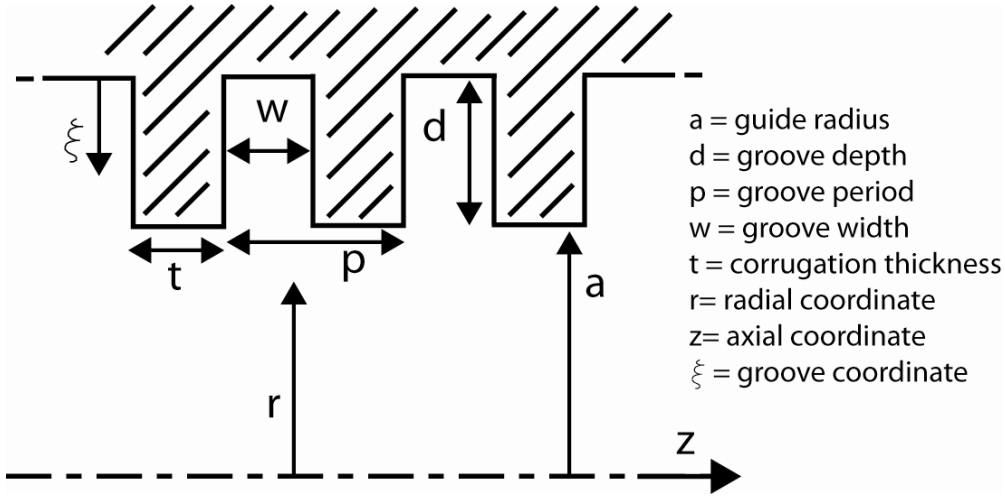

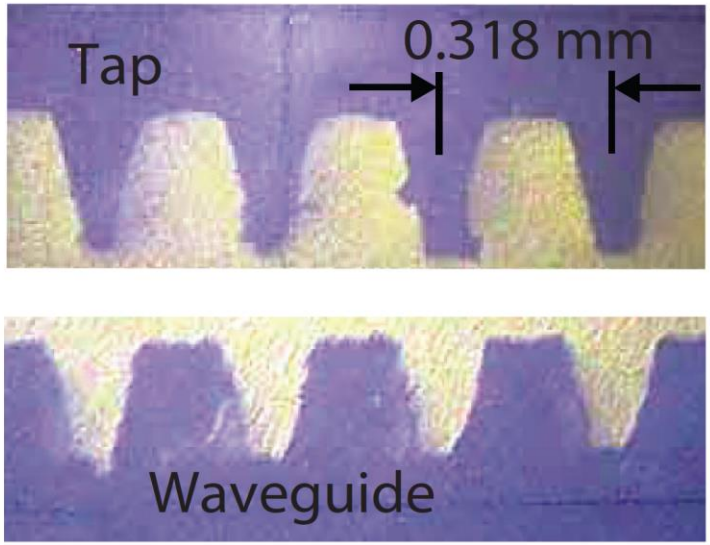

Nanni et al., JIMT, July 2012, Volume 33, Issue 7, pp 695-714

Impedance Approximation

- Impedance of the corrugations determined by the groove geometry
- Corrugations behave like a shorted transmission line for *d=λ/4* impedance at surface wall is infinite resulting in a null for the magnetic field
- $$Z = \frac{w}{p} \tan kd$$

$$\mathbf{H}(r = a, \phi) = \mathbf{h}_{01} = -\left(\frac{1}{Z_0 \pi}\right)^{1/2} \frac{\chi_m}{ka^2} \left[\hat{\phi} \frac{1}{Z}\right]$$

- Magnetic field inside the groove

$$h_\phi \frac{\cos k\xi}{\cos kd} \qquad 0 \le \xi \le d$$

Loss Measurements

- Loss can be very low even at hundreds of GHz
- Measured loss of 0.029±0.009 dB/m at 250 GHz (improved to 0.01 dB/m)

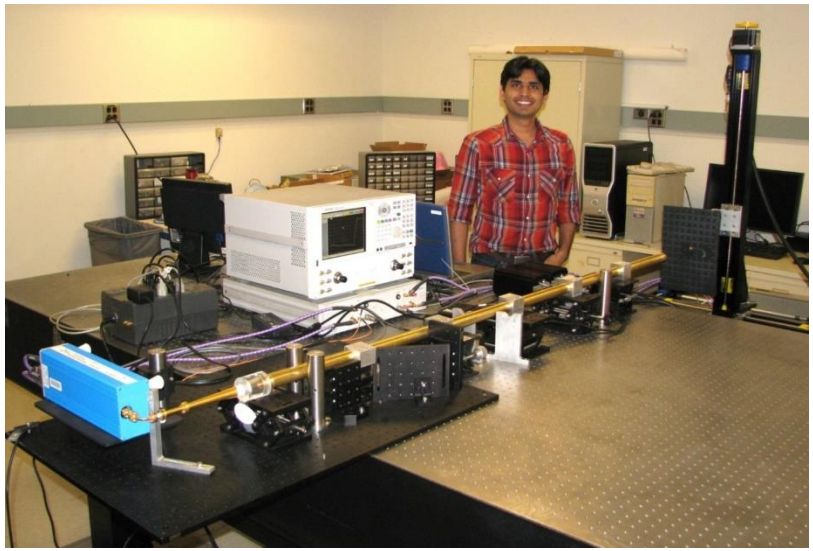

Far Field Pattern

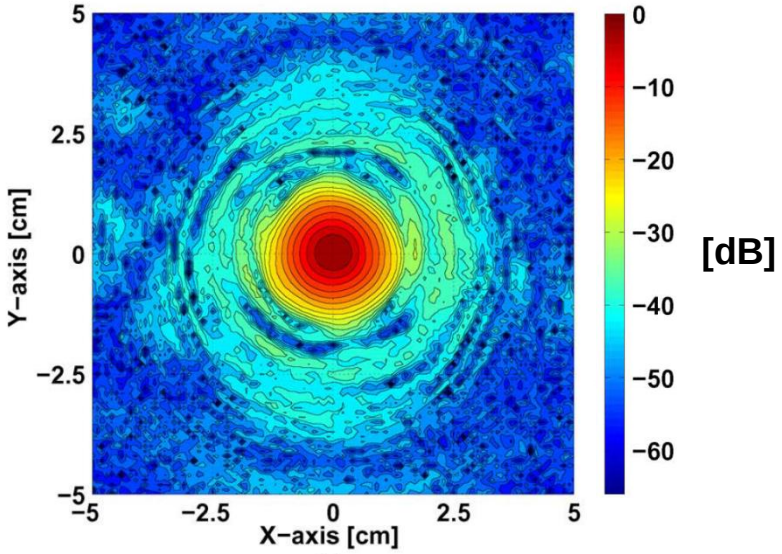

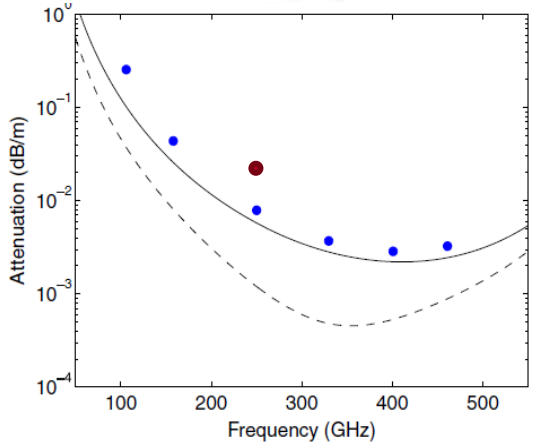

Nanni et al., JIMT, July 2012, Volume 33, Issue 7, pp 695-714

X-band Structure: Hybrid Mode Fields

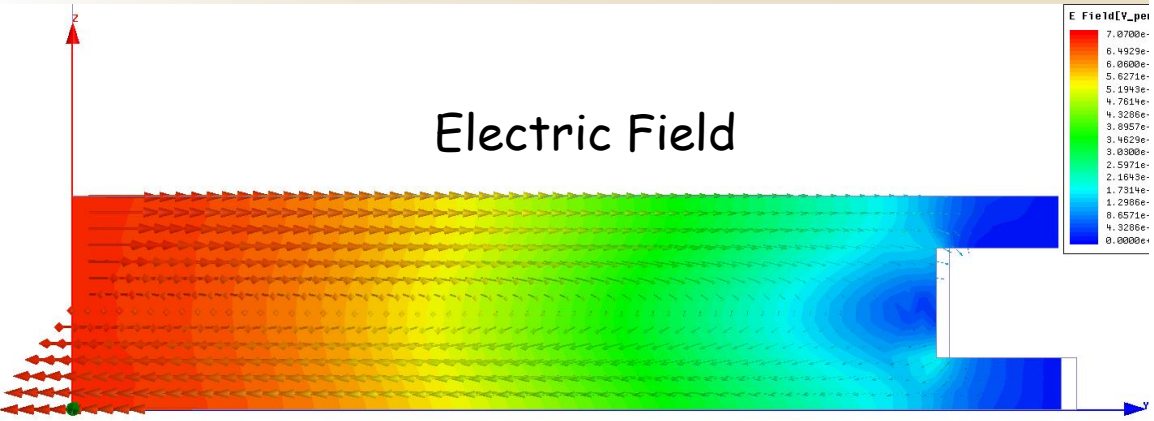

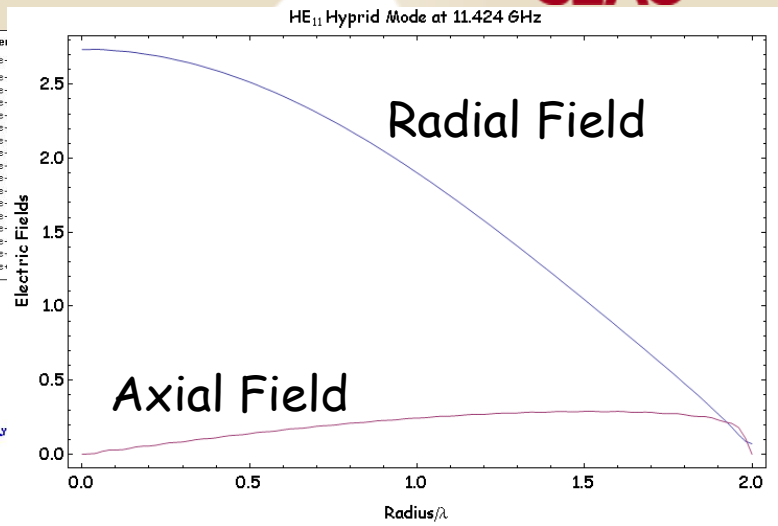

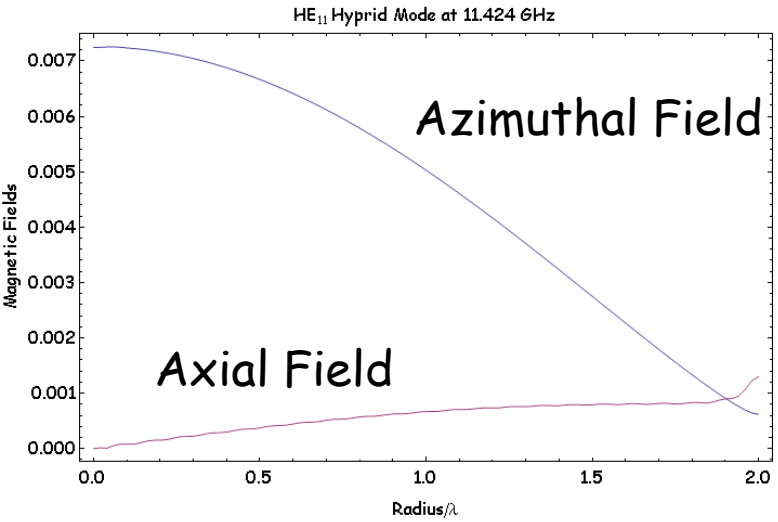

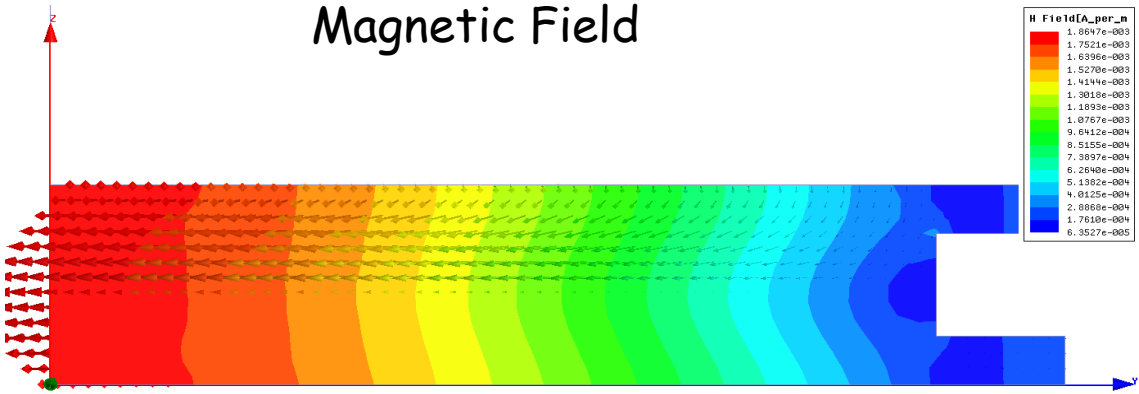

Slide: S. Tantawi

HE_{1n} Modes Scaling Laws

For an undulator made of copper at room temperature :

$$\lambda_u \approx \frac{\lambda}{2}$$

$$Power: \quad P(MW) \approx K^2 J_1^{\,2}(x)\left(\frac{0.727141a^2}{\lambda_u^{\,5/2}} + \frac{0.0673433Lx^2}{a\sqrt{\lambda_u}}\right)$$

$$Stored\ Energy: \quad U(Jouls) \approx \frac{71.5a^2K^2LJ_1^{\,2}(x)}{\lambda_u^2}$$

$$Quality\ Factor: \quad Q \approx \frac{1.17\times10^8 a^3 L}{128\pi^2a^3 + 117Lx^2\lambda_u^2}\sqrt{\frac{1}{\lambda_u}}$$

$$Filling\ Time: \quad t_f(\mu s) \approx \frac{124208\ a^3L\sqrt{\lambda_u}}{\left(128\pi^2a^3 + 117Lx^2\lambda_u^2\right)}$$

$$Peak\ Suface\ E\ Field: \quad E_s(MV/m) \approx \frac{1.02KxJ_1(x)}{a}$$

$$Peak\ Surface\ B\ Field: B_s(mT) \approx \frac{3.4KxJ_{1.}(x)}{a}$$

$$x \to \{2.40483, 5.52008, 8.65373, 11.7915\}\ for\ \{HE_{11}, HE_{12}, HE_{13}, HE_{14}\}\ modes$$

Slide: S. Tantawi

Undulator Coupler Design

Two coupling ports 90° apart to excite two polarizations independently

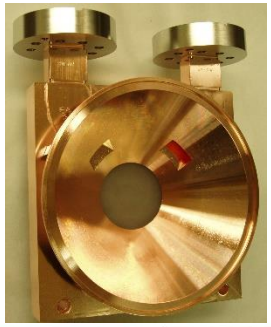

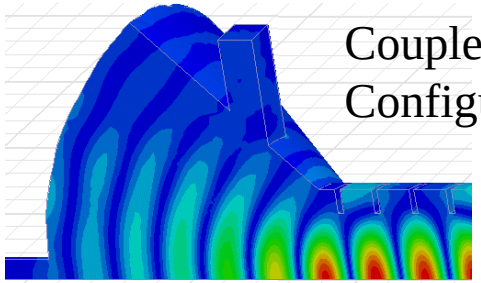

Coupler Field Configuration

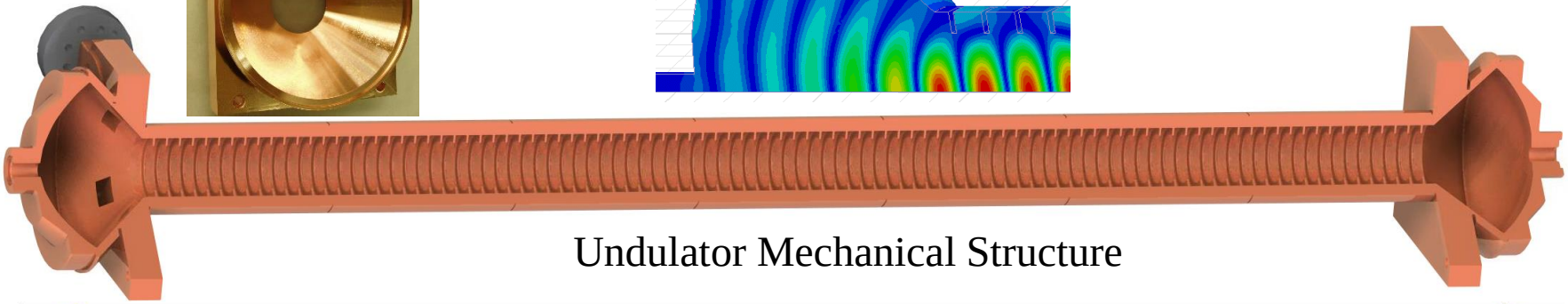

Undulator Mechanical Structure

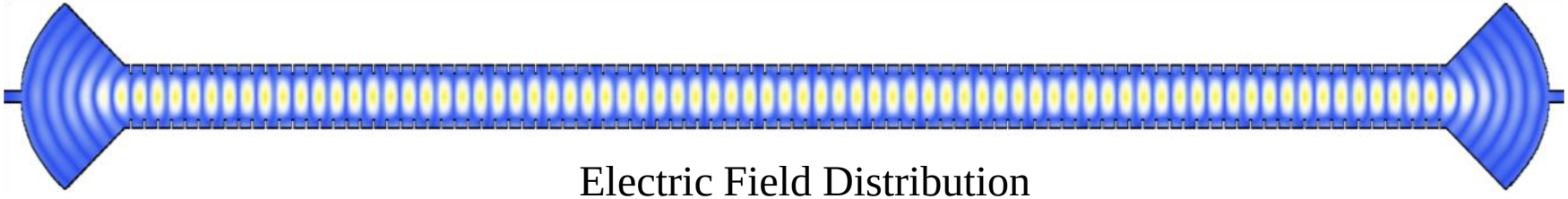

Electric Field Distribution

Corrugation Period=0.4254 λ
Inner Radius=0.75 λ
Outer radius= 1.01293 λ
Corrugation Thickness= λ/16
Number of periods =98

λ=2.6242296 cm
Undulator Wavelength=1.39306 cm
Power required (for linearly polarized, K=1)=48.8 MW
Q0=94,000

Slide: S. Tantawi

Undulator Structure Tested at NLCTA

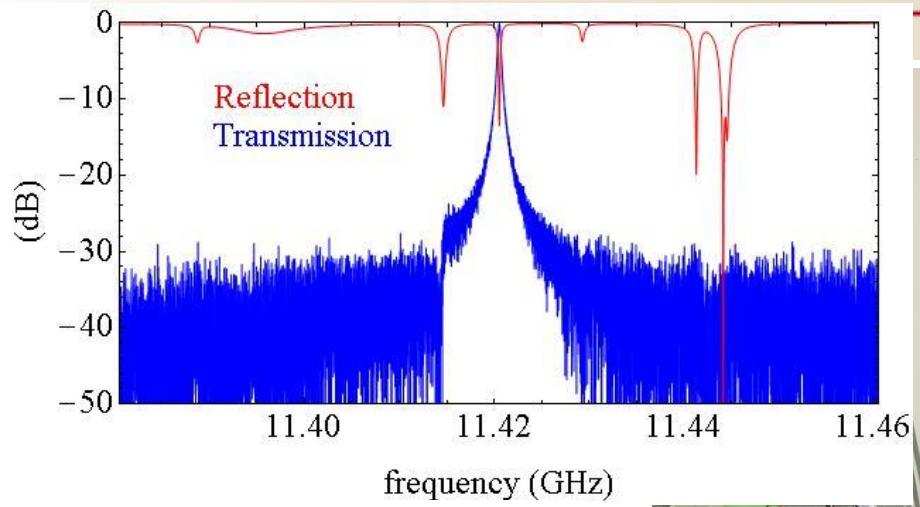

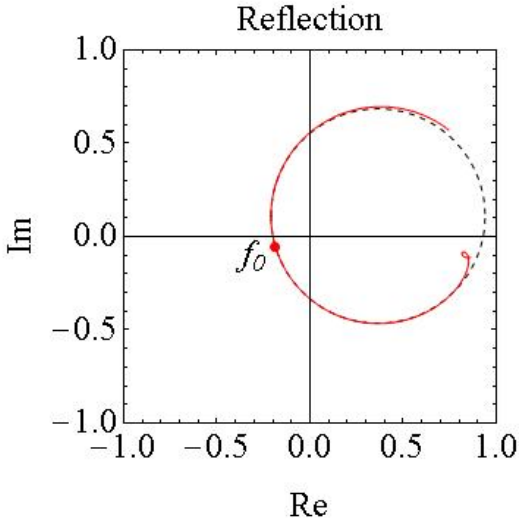

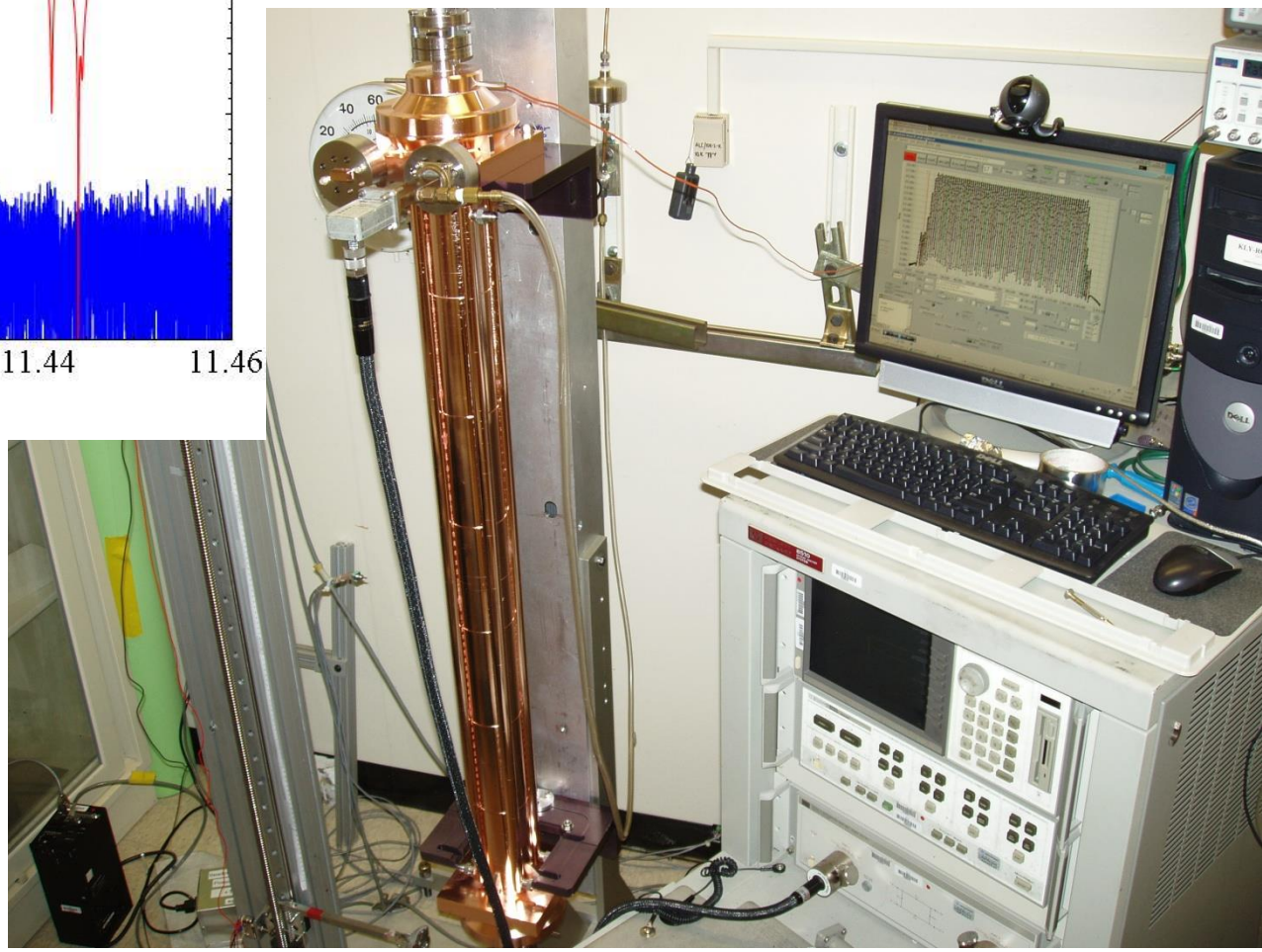

Calculations from cold test data @ 20 °C with air:

Resonance Frequency (f_0) = 11.419 GHz (11.424 under vacuum @12.1 °C)

β = 1.53, $Q_0 = (1+\beta)\, Q_{total}$ = 91,000 (Simulations 94,000)

Slide: S. Tantawi

Comparison between Simulations and Cold Test Data

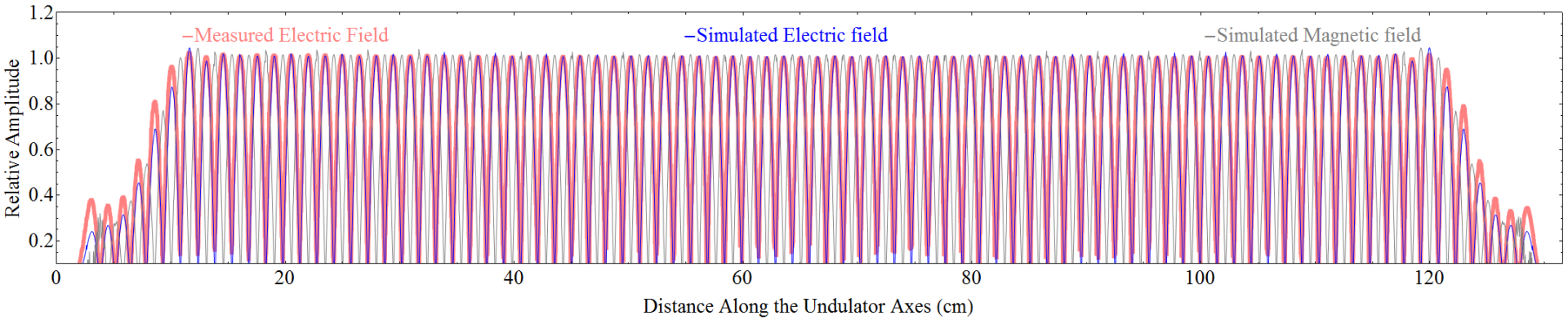

Tantawi, Sami, et al. "Experimental demonstration of a tunable microwave undulator." *Physical review letters* 112.16 (2014): 164802.

Slide: S. Tantawi

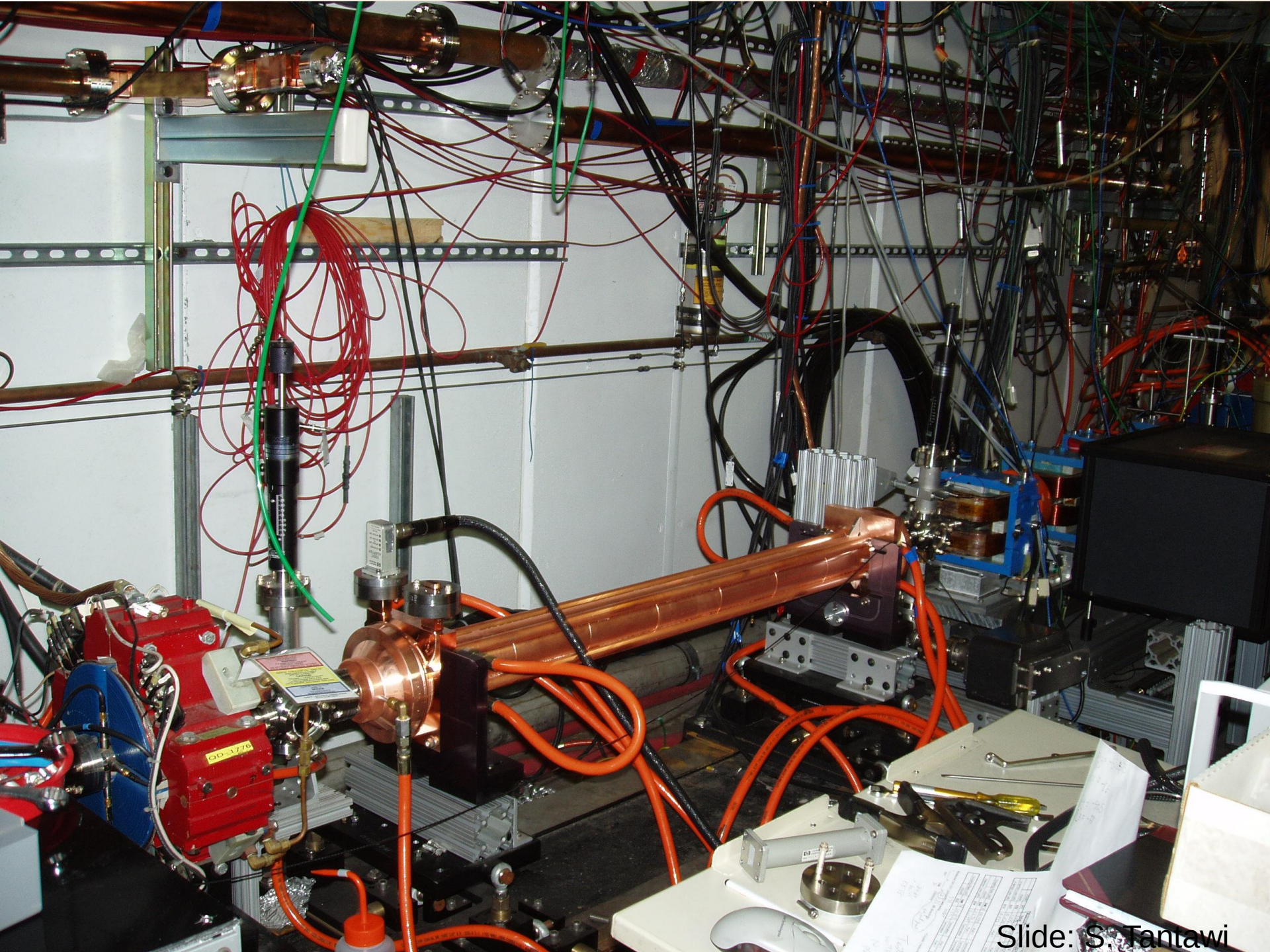
Slide: S. Tantawi

Technologies of Interest to Axion Community

SLAC

Coupled Cavity Structures

Mode Selective Cavities

Low Loss Waveguides and Cavities

Low Temperature Surface Resistivity Measurements

Advanced superconducting material testing setup

- New, 2nd generation cryostat dedicated to SRF materials characterization.
- Improvements over 1st gen.:
  - Remote-motor cryocooler – to reduce cavity vibrations and fluctuations in resonant frequency.
  - Increased pumping – to improve cryostat base pressure (1e-9 torr vs. 1e-6 torr prior).
  - Improved thermal isolation – to increase 4 K cooling power reserved for cavity dissipation.

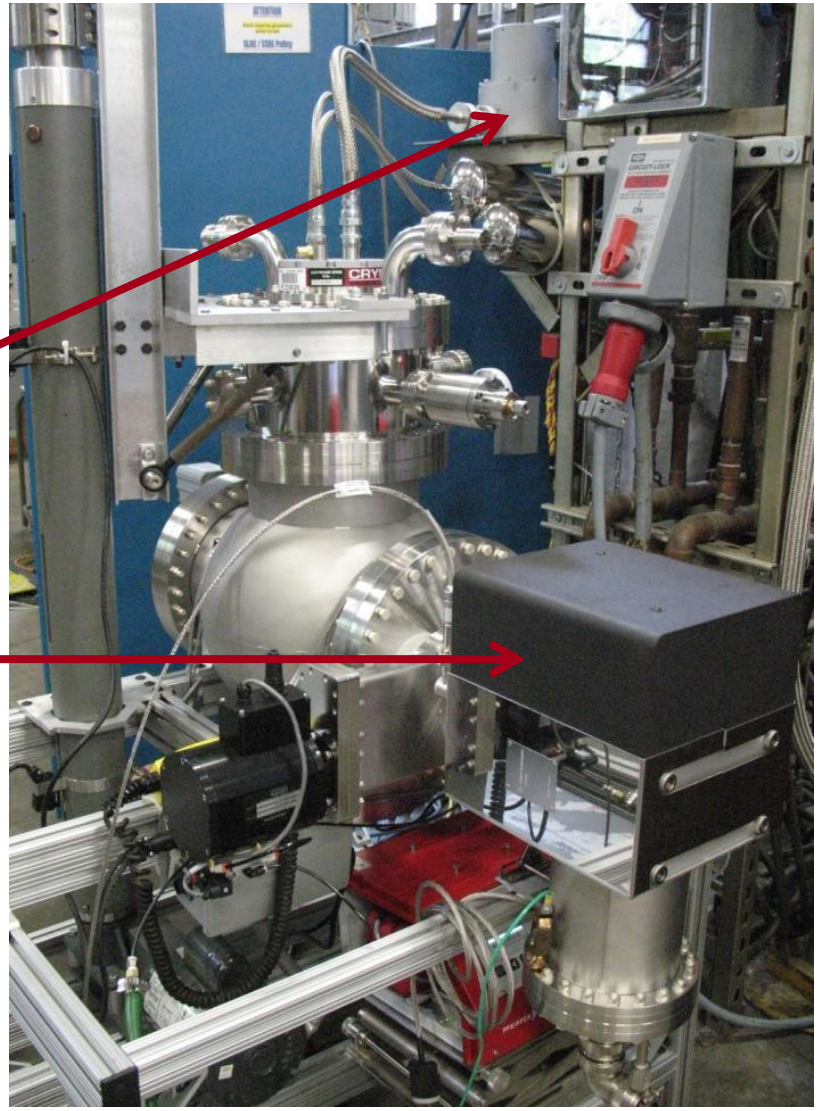

Slide: S. Tantawi

Basic Calculations

- Use measurement of **Q** and HFSS calculation of **G** to determine **R**

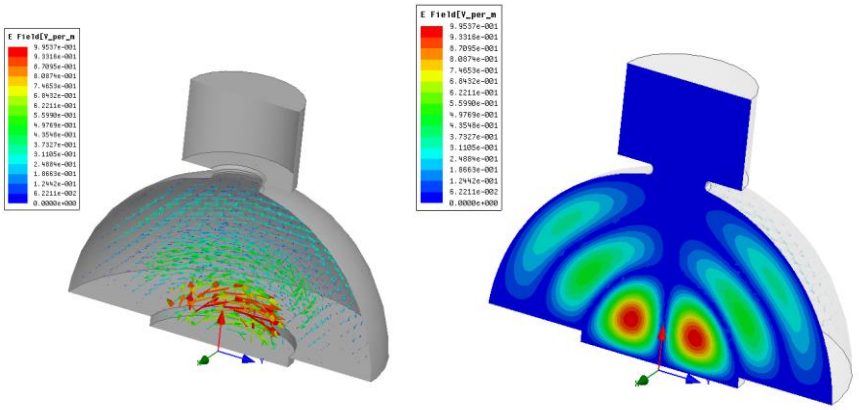

Geometric Factors:

G_{total} =1388.7
G_{sphere} =2066.5
G_{sample}=4233.1

$$G = R_s Q_0 = \omega \mu_0 \frac{\int\int\int |H|^2 dV}{\int\int |H|^2 dA}$$

$$\frac{1}{G_{total}} = \frac{1}{G_{sphere}} + \frac{1}{G_{sample}}$$

$$R_{s_{sample}} = \frac{G_{sample}}{Q_{sample}} = G_{sample}\left(\frac{1}{Q_0} - \frac{R_{s_{Ni}}}{G_{sphere}}\right)$$

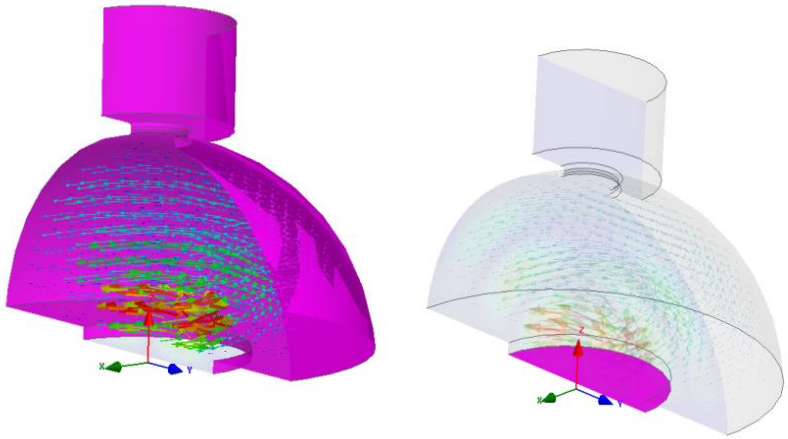

Sphere Surface Sample Surface

Slide: P. Welander and M. Franzi

Guo, Jiquan, et al. "Cryogenic RF Material Testing at SLAC." PAC, 2011.

High-Power Testing

- Utilizes Cu cavity and XL-4 klystron as RF source.
  - Cu does not quench like a superconductor
  - **H**-field on the sample surface is roughly quadratic with radius
  - Sample quenches gradually, with the normal ring growing wider with increasing power

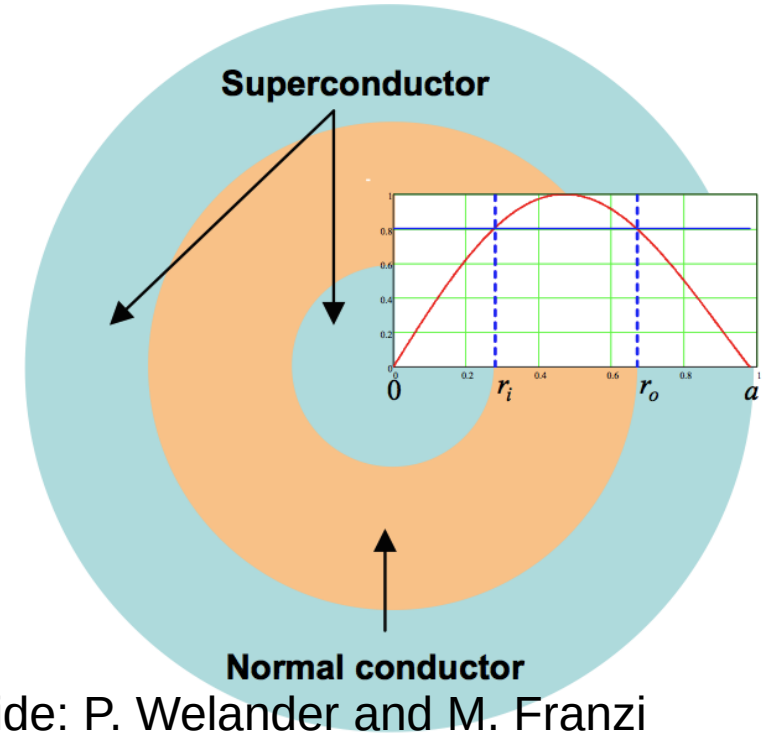

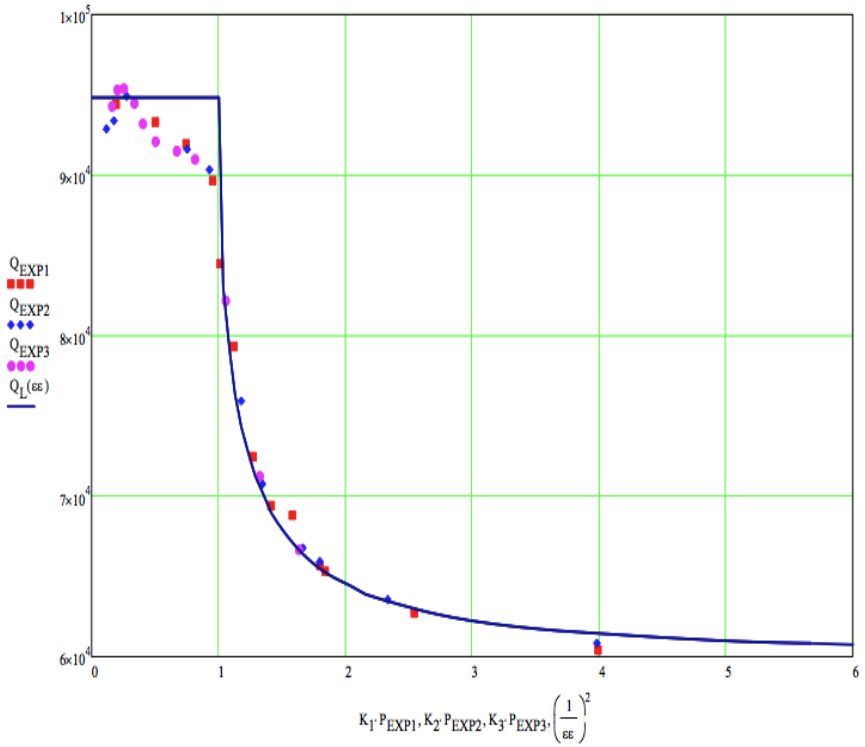

Slide: P. Welander and M. Franzi

Low-Power Testing in Cu Cavity

- With a programmable network analyzer (PNA) as power source, measure S_{22} parameter.
  - Copper has no transition temperature, making it ideal for measuring sample T_c

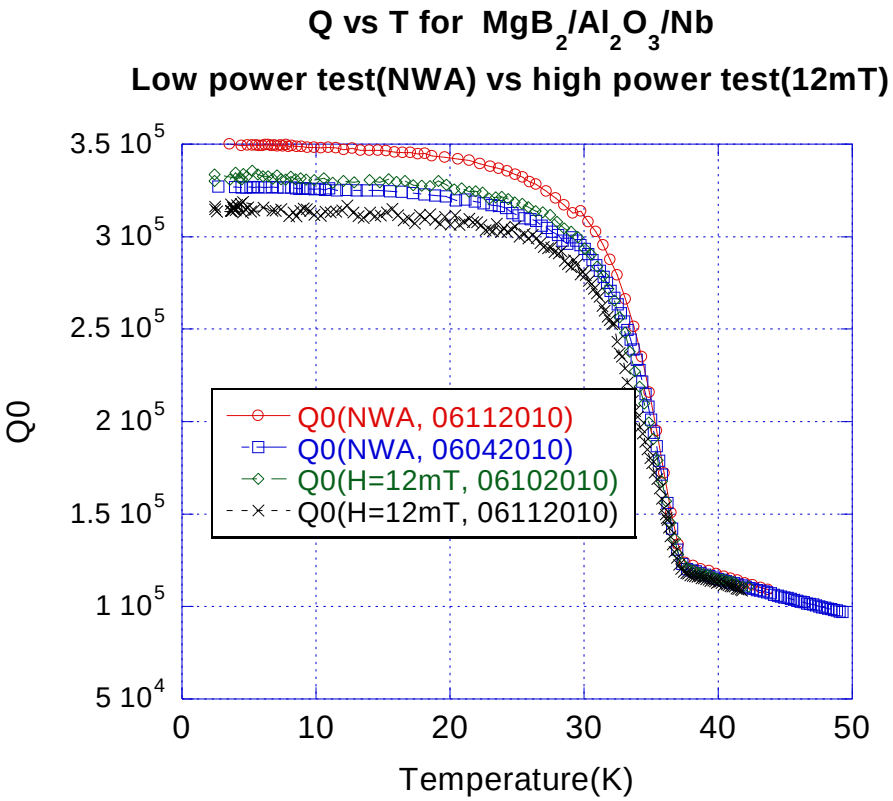

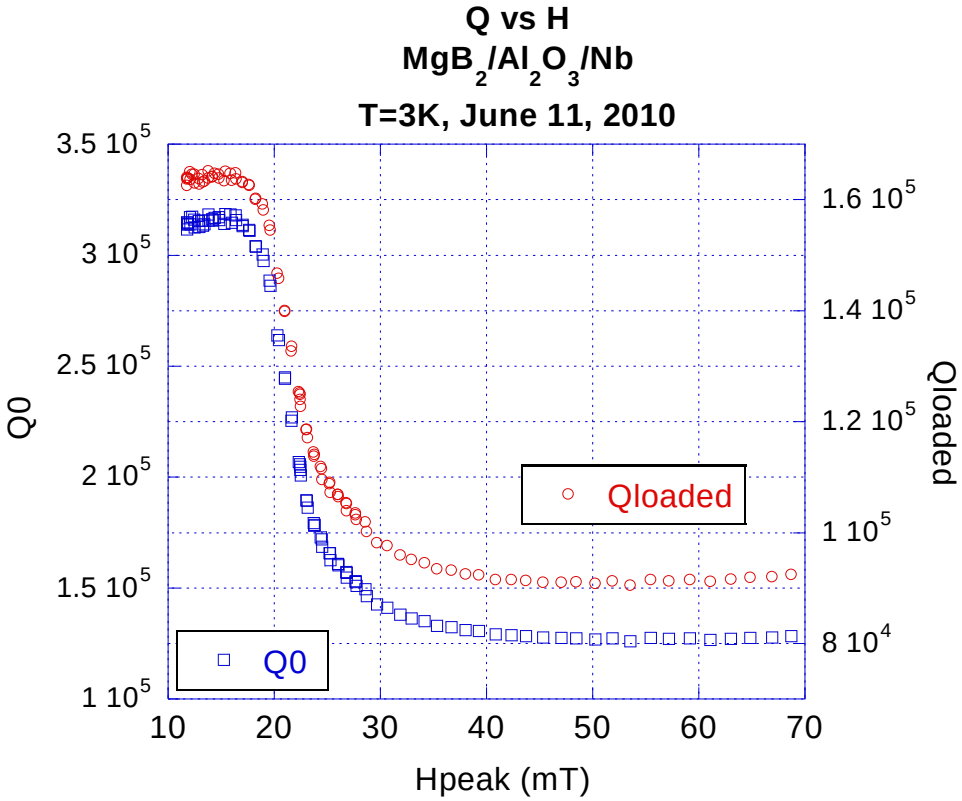

Slide: P. Welander and M. Franzi

Questions?